

Active Thermal Control of Distributed Parameter Systems Excited at Multiple Frequencies

Christoph C. Richter

Institut für Thermodynamik,
Technische Universität Braunschweig,
Hans-Sommer-Straße 5,
38106 Braunschweig, Germany
e-mail: ch.richter@tu-bs.de

John H. Lienhard V

Department of Mechanical Engineering,
Massachusetts Institute of Technology,
77 Massachusetts Avenue, Room 3-162,
Cambridge, MA 02139-4307
e-mail: lienhard@mit.edu

In testing packaged high-power integrated circuits, active thermal control is useful in providing die-level temperature stability. A time-varying heat load is applied to the surface of the package to compensate for the time-varying test power sequence applied to the die. An earlier study determined the proper control heat load for a single-frequency sinusoidal variation in die power subject to a finite allowed temperature variation on the die. Actual test power sequences contain many frequencies at various phase angles, each contributing to the temperature variation of the die. In the present study, we develop a method of controlling multiple frequency test sequences subject to a finite temperature tolerance. It is shown that the total control power may be minimized assigning temperature tolerances to the highest frequencies in the test power sequence. [DOI: 10.1115/1.2130408]

Keywords: conduction, control, electronics, heat transfer, temperature

1 Introduction

Precise temperature control of high-power microprocessor devices during testing is very important in order to properly classify the device performance [1]. The device manufacturer specifies a temperature and an allowed deviation from it during the testing procedure (e.g., 85°C–0/+2°C). A temperature deviation larger than the prescribed one might lead to an improper classification of the tested integrated circuit device (e.g., a 2 GHz device is classified as a 1.8 GHz device) due to reduced signal propagation speeds at higher temperatures [2]. The test process applies computer-controlled electrical signals to the device, and, for high-power devices, this may result in die-average power density in the range of 100 kW/m². The frequency components of the die-average power that are energetic enough to affect die temperature range from zero to a hundred hertz or so.

Feedback control of the die temperature is usually not possible, owing to the lack of an accessible die-level temperature sensor. An alternative approach to thermal management in automatic testing equipment was proposed and tested by Sweetland, Lienhard, and Slocum [2,3]. In this approach, the surface of the device under test is heated with laser radiation while simultaneously cooled by

forced convection. Through modulation of the laser power, the device temperature can be dynamically stabilized to within a set tolerance.

A significant complication in this scheme arises from the time required for temperature signal propagation from the device package surface to the die, upon which the power is actually dissipated. Figure 1 provides a cross-sectional view of a typical high-power microprocessor device. Sweetland and Lienhard [4] analyzed the effect of the conductive time lag on the control power for sinusoidal die power, showing that it tends to increase the required laser power substantially, and leads to optical powers several times larger than the die power. Minimization of the required laser power, which can amount to hundreds of watts or more, is of great importance in order to limit both the electrical power consumed by the control system and the added load on the test facility's cooling system.

This paper extends the analysis of Sweetland and Lienhard [4] to multifrequency waveforms, with the aim of determining optimal control power for multifrequency test power sequences. We show that the control profile calculation with specified die temperature tolerance presented in [4] is not suitable for nonsinusoidal die power profiles, and we develop a new approach for this situation.

2 Single Frequency Die Power Profiles

The mathematical method follows the one-dimensional model of Sweetland and Lienhard [4]. Figure 1 shows a typical cross section of a high-power microprocessor device. For transient response, the physical model of such a device is reduced to the one-dimensional model shown in Fig. 2 as detailed in [4]. The most important parts for the thermal analysis are the silicon die and the integrated heat spreader (IHS) which is typically made from plated copper. A thin layer of a thermal interface material or grease is used to optimize the heat exchange between die and IHS. As in the previous work, the interface material is taken to have thermal resistance, but negligible heat capacity; and losses to the device substrate are set to zero, giving an upper bound on control power. As in the earlier study, die's heat generation is taken to be uniform over its area, so that attention may be focused on the analysis of frequency effects on the control scheme (see [5] for numerical studies of nonuniform die heating).

The steady periodic transient response can be found using a complex temperature approach [6]. All steady components of power and temperature may be set to zero, by superposition, and attention will be directed to the time-varying response. It is assumed that the solution to the temperature profile in the complex plane takes the form

$$W(x,t) = X(x)e^{i\omega t} \quad (1)$$

where $i = \sqrt{-1}$ is the imaginary number and ω is the frequency of die power variation; x is measured from the convection side of the IHS. The one-dimensional conduction equation in the IHS can be written

$$\frac{\partial^2 W(x,t)}{\partial x^2} = \frac{1}{a_t} \frac{\partial W(x,t)}{\partial t} \quad (2)$$

where a_t is the thermal diffusivity of the IHS material. The general solution for this equation is known to be

$$X(x) = c_1 e^{-xL(i+1)} + c_2 e^{xL(i+1)} \quad (3)$$

where $L \equiv \sqrt{\omega/2a_t}$ is the unsteady diffusion scale in the IHS.

2.1 IHS Temperature Response. The transient temperature response of the IHS can be found by decomposing the model shown in Fig. 2 into two subsystems and superimposing the results [4], removing all steady components of optical heating, cooling, and die heating. The transient component of die power is a single frequency profile of the form

Contributed by the Heat Transfer Division of ASME for publication in the JOURNAL OF HEAT TRANSFER. Manuscript received August 4, 2004; final manuscript received February 10, 2005. Review conducted by Ramendra P. Roy.

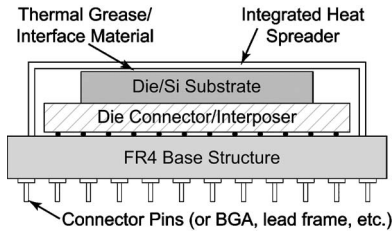


Fig. 1 Typical cross section of a high-power microprocessor device

$$q_d(t) = Q_d \cos(\omega t) \quad (4)$$

where Q_d is the die power density. In this first step of the analysis, the die power is applied directly to the die side of the IHS ignoring the influences of the die and the thermal interface material. The convection side of the IHS is subject to convective boundary conditions, an average heat transfer coefficient h_c with an air temperature $T_{\text{air}}=0$ K, by superposition, and a control power flux

$$q_c(t) = Q_c \cos(\omega t + \alpha) \quad (5)$$

where Q_c is the control power density and α is a phase shift. Of special interest is the die side or back-face (BF) temperature of the IHS which can be found to be

$$\begin{aligned} T_{\text{BF}}(t) = & \frac{2Q_c e^{bL}}{kL(A^2 + B^2)} \{ [A \cos \alpha + B \sin \alpha] \cos(\omega t) \\ & + [B \cos \alpha - A \sin \alpha] \sin(\omega t) \} + \frac{Q_d e^{-bL}}{kL(P^2 + R^2)} \{ [U \cos(bL) \\ & + V \sin(bL)] \cos(\omega t) + [U \sin(bL) - V \cos(bL)] \sin(\omega t) \} \\ & + \frac{Q_d e^{bL}}{kL(P^2 + R^2)} \{ [P \cos(bL) + R \sin(bL)] \cos(\omega t) \\ & + [R \cos(bL) - P \sin(bL)] \sin(\omega t) \} \end{aligned} \quad (6)$$

where b is the IHS thickness and k its thermal conductivity. A , B , P , R , U , and V are mathematical constants as defined in [4] and are given in the Appendix. It should be noted that the constants only depend on bL , which is a dimensionless frequency parameter, and the Biot number for the convection side of the IHS, $\text{Bi}_{\text{IHS}}=h_c b/k$.

2.2 Temperature Response of Die. The die normally has small thermal resistance and can be treated as isothermal for the frequencies of interest. Its temperature response can be described by a lumped capacitance model [4]

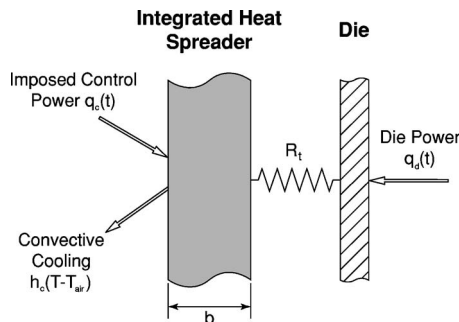


Fig. 2 Schematic diagram of simplified device for transient analysis

$$m c_p \frac{dT_{\text{DIE}}}{dt} = Q_d \cos(\omega t) - \frac{T_{\text{DIE}} - T_{\text{BF}}}{R_t} \quad (7)$$

where m is the die mass per unit area and c_p is the specific heat capacity of the die at constant pressure; R_t is the thermal contact resistance of the interface material. This equation neglects the heat capacity of the thermal interface material between the die and the IHS. The die is lumped because the Biot number $b_{\text{DIE}}/(R_t k_{\text{DIE}})$ is small (in the example below, its value is 0.032).

For ideal die temperature control [$T_{\text{DIE}}(t)=\text{const}$ and $dT_{\text{DIE}}/dt=0$], Eq. (7) can be written as

$$T_{\text{BF}}(t) = -Q_d R_t \cos(\omega t) \quad (8)$$

where the steady component T_{DIE} is set to zero, again by superposition. To compute the control power density amplitude and phase shift Q_c and α that are required to produce the IHS back-face temperature given in Eq. (8), Eq. (6) can be used. The result is

$$\begin{aligned} & \left\{ \frac{2Q_c e^{bL}}{A^2 + B^2} [A \cos \alpha + B \sin \alpha] + C_1 Q_d + Q_d k L R_t \right\} \cos(\omega t) \\ & + \left\{ \frac{2Q_c e^{bL}}{A^2 + B^2} [B \cos \alpha - A \sin \alpha] + C_2 Q_d \right\} \sin(\omega t) = 0 \end{aligned} \quad (9)$$

with the additional definitions

$$C_1 = \frac{e^{-bL} [U \cos(bL) + V \sin(bL)] + e^{bL} [P \cos(bL) + R \sin(bL)]}{P^2 + R^2} \quad (10)$$

$$C_2 = \frac{e^{-bL} [U \sin(bL) - V \cos(bL)] + e^{bL} [R \cos(bL) - P \sin(bL)]}{P^2 + R^2} \quad (11)$$

Equation (9) must hold true for any time t . Therefore, the sine and cosine terms have to vanish separately. Using this requirement, the phase shift α can be computed as

$$\alpha = \arctan \left(\frac{C_1 B + B k L R_t - C_2 A}{C_2 B + A k L R_t + C_1 A} \right) \quad (12)$$

The phase shift α is always picked so that the control power density, Q_c , becomes positive

$$Q_c = - \frac{A^2 + B^2}{2e^{bL} [A \cos \alpha + B \sin \alpha]} \{ C_1 + k L R_t \} Q_d \quad (13)$$

2.3 Control Profile Calculation With Specified Die Temperature Tolerance. Sweetland and Lienhard [4] assume in their analysis a back-face IHS temperature profile $T_{\text{BF}}(t)$ and use this profile to compute the optimal control power for control to a prescribed temperature tolerance. This method yields a small control power density but not the optimal control power density. Instead of assuming a back-face IHS temperature, the die temperature profile $T_{\text{DIE}}(t)$ is assumed to be

$$T_{\text{DIE}}(t) = \frac{\Delta T}{2} \cos(\omega t + \beta) \quad (14)$$

where ΔT is the prescribed temperature tolerance for the device under test (ΔT is defined as the peak-to-peak amplitude of the die temperature profile to be consistent with [4]) and β is an unknown phase shift. In order to compute the control power profile, the back-face IHS temperature profile has to be known. This profile can be computed by using Eq. (14) in Eq. (7) and rearranging the resulting equation to T_{BF}

$$T_{BF}(t) = - \left\{ \frac{\omega \Delta T}{\lambda} \frac{\Delta T}{2} \cos \beta + \frac{\Delta T}{2} \sin \beta \right\} \sin(\omega t) - \left\{ \frac{\omega \Delta T}{\lambda} \frac{\Delta T}{2} \sin \beta - \frac{\Delta T}{2} \cos \beta + Q_d R_t \right\} \cos(\omega t) \quad (15)$$

where $\lambda = 1/mc_p R_t$ ($1/\lambda$ is the lumped-capacity time constant associated with Eq. (7)). To derive Eq. (6) it was assumed that the die power is applied at the back face of the IHS neglecting the thermal contact resistance R_t . Equation (7) can be used to find the actual heat flux from the die into the IHS. This heat flux takes on the form

$$q_{BF}(t) = Q_{BF} \cos(\omega t + \gamma) \quad (16)$$

with

$$Q_{BF} = \frac{1}{2} \sqrt{4Q_d^2 + 4Q_d \omega mc_p \Delta T \sin \beta + (\omega mc_p \Delta T)^2} \quad (17)$$

$$\gamma = \arctan \left(- \frac{\omega mc_p \Delta T \cos \beta}{\omega mc_p \Delta T \sin \beta + 2Q_d} \right) \quad (18)$$

Using this corrected heat flux, Eq. (6) can be written as

$$T_{BF}(t) = \left\{ \frac{2Q_c e^{bL}}{A^2 + B^2} [A \cos \alpha + B \sin \alpha] + \frac{kL}{\lambda} \omega \frac{\Delta T}{2} \sin \beta - kL \frac{\Delta T}{2} \cos \beta + Q_d kLR_t + (C_1 + C_2 \tan \gamma) \left(Q_d + \omega mc_p \frac{\Delta T}{2} \sin \beta \right) \right\} \cos(\omega t) + \left\{ \frac{2Q_c e^{bL}}{A^2 + B^2} [B \cos \alpha - A \sin \alpha] + \frac{kL}{\lambda} \omega \frac{\Delta T}{2} \cos \beta + kL \frac{\Delta T}{2} \sin \beta + (C_2 - C_1 \tan \gamma) \left(Q_d + \omega mc_p \frac{\Delta T}{2} \sin \beta \right) \right\} \sin(\omega t) \quad (19)$$

This equation has to hold true for any time t , which yields a phase shift α

$$\alpha = \arctan \left(\frac{-(C_2^* \lambda B + C_1^* \omega A) \Delta T \cos \beta + (C_1^* \omega B - C_2^* \lambda A) \Delta T \sin \beta + (C_1 B + B kLR_t - C_2 A) \lambda 2Q_d}{(C_1^* \omega B - C_2^* \lambda A) \Delta T \cos \beta + (C_2^* \lambda B + C_1^* \omega A) \Delta T \sin \beta + (C_2 B + A kLR_t + C_1 A) \lambda 2Q_d} \right) \quad (20)$$

where C_1^* and C_2^* are defined as

$$C_1^* = kL + \lambda mc_p C_1 \quad \text{and} \quad C_2^* = kL + \omega mc_p C_2 \quad (21)$$

The control power for this control case can be computed by substituting Eq. (20) into

$$Q_c = - \frac{A^2 + B^2}{2e^{bL} [A \cos \alpha + B \sin \alpha]} \left\{ \frac{kL}{\lambda} \omega \frac{\Delta T}{2} \sin \beta - kL \frac{\Delta T}{2} \cos \beta + Q_d kLR_t + (C_1 + C_2 \tan \gamma) \left(Q_d + \omega mc_p \frac{\Delta T}{2} \sin \beta \right) \right\} \quad (22)$$

which is derived from Eq. (19) by forcing sine and cosine terms to vanish separately. The phase shift α is again picked so that the control power density Q_c becomes positive.

The solution for α and Q_c is still dependent on the unknown phase shift β . To find the optimal control power, Eq. (22) has to be minimized with respect to β . This can be done by substituting Eq. (20) into Eq. (22) and setting the first derivative with respect to β of this equation to zero. This yields

$$\beta = - \arctan \left(\frac{[\omega C_1 + \lambda C_2 + (kL + \lambda mc_p C_1) \omega R_t] kL + \omega mc_p (C_1^2 + C_2^2) \lambda}{[\lambda C_1 - \omega C_2 + (kL + \omega mc_p C_2) \lambda R_t] kL} \right) \quad (23)$$

Using this equation for β in Eq. (20) simplifies the phase shift α to

$$\alpha = \arctan \left(\frac{C_1 B + B kLR_t - C_2 A}{C_2 B + A kLR_t + C_1 A} \right) \quad (24)$$

This phase shift is identical to that previously derived for control at constant die temperature (Eq. (12)): The resulting phase shift is not dependent on the prescribed temperature tolerance ΔT . Using Eq. (22) and setting the control power density to zero ($Q_c = 0 \text{ W/m}^2$), allows us to compute the maximal temperature fluctuation (peak-to-peak) for a given die power profile, which occurs when no control power is applied

$$\Delta T_{\max} = \frac{(kLR_t + C_1) \lambda 2Q_d}{(kL + \omega mc_p C_2) \lambda \cos \beta - (kL + \lambda mc_p C_1) \omega \sin \beta} \quad (25)$$

It is interesting to note that the control power density Q_c is linearly dependent on the prescribed temperature tolerance ΔT for the optimal control case

$$Q_c = Q_{c0} - Q_{c1} \Delta T \quad (26)$$

where

$$Q_{c0} = - \frac{A^2 + B^2}{2e^{bL} [A \cos \alpha + B \sin \alpha]} \{C_1 + kLR_t\} Q_d \quad (27)$$

$$Q_{c1} = \frac{A^2 + B^2}{4e^{bL} [A \cos \alpha + B \sin \alpha]} \left\{ \left(kL \frac{\omega}{\lambda} + \omega mc_p C_1 \right) \sin \beta - (kL + \omega mc_p C_2) \cos \beta \right\} \quad (28)$$

The constant part of the control power density Q_{c0} is the control power that has been calculated previously for control to constant die temperature (Eq. (13)). The linear coefficient Q_{c1} is not dependent on the die power density, Q_d , but will increase with an increase in the frequency of die power fluctuation ω . This result is of special importance for the discussion of nonsinusoidal control power profiles.

Using the method presented in [4] to compute the optimal control profile for a prescribed temperature tolerance, the phase shift β was found to be

$$\beta = \arctan(-\omega mc_p R_t) \quad (29)$$

This phase shift will yield a small, but not optimal, control power density as can be seen in the following example.

Example. A dimensional example for the control of a single-

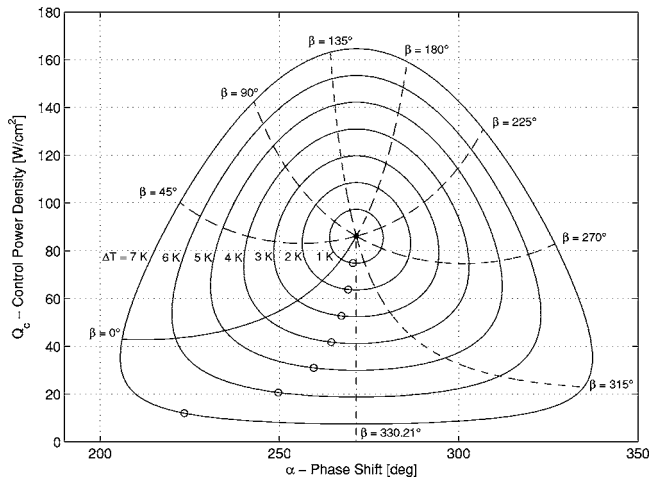


Fig. 3 Control power densities and phase shifts for single frequency die power profile ($\omega=5$ Hz and $Q_d=10$ W/cm²) and multiple prescribed temperature tolerances ΔT . The problem properties are given in Tables 1 and 2. The circles \circ mark the points computed using the method given in [4].

frequency die power profile to a prescribed temperature tolerance is given in Fig. 3. The material data for this example is given in Table 1, and further properties, including the geometry, are presented in Table 2. (The geometrical values are representative and are chosen only for purposes of illustration.) The die power profile is given by Eq. (4) with a frequency of 5 Hz and a die power density magnitude of $Q_d=10$ W/cm². The prescribed temperature tolerance is varied from 0 K to 7 K in increments of 1 K. The center point in Fig. 3 marks the solution for a constant die temperature $\Delta T=0$. Every ring around this center point represents the solution for a single prescribed temperature tolerance and phase shifts $0 \leq \beta \leq 2\pi$. The optimal solution is represented by the vertical line at $\beta=330.21$ deg: Note that the intersection points of the optimal solution and the rings are equally spaced; this follows from Eq. (26). The points computed using the method proposed by Sweetland and Lienhard [4] are marked with circles. It can be seen that they are relatively close to the optimal solution in terms of the control power density Q_c but yield different phase shifts α . The maximal temperature fluctuation for this example can be computed from Eq. (25), giving $\Delta T_{\max}=7.67$ K.

Figure 4 shows the effect of die power frequency variation on the required control power. The upper line indicates the control power needed to obtain a constant die temperature Q_{c0} . This power grows rapidly with rising frequency due to the fact that the thermal mass of the IHS has to be driven over the same temperature difference faster at higher die power frequency. Clearly, control to zero fluctuation will become impractical owing to the very high control powers required. Commercially available diode lasers

Table 1 Material properties for examples

Material	Density	Specific Heat	Thermal Conductivity
Copper (IHS)	8950 kg/m ³	385 J/kg·K	386 W/m·K
Silicon (Die)	2330 kg/m ³	699 J/kg·K	148 W/m·K

Table 2 Problem properties and geometry for examples

Problem Properties			Geometry	
Average heat transfer coefficient	h_c	1200 W/m ²	IHS thickness	b 1.8 mm
Thermal contact resistance	R_t	0.42 K·cm ² /W	Die thickness	b_{DIE} 0.2 mm
Air temperature	T_{air}	0 K		

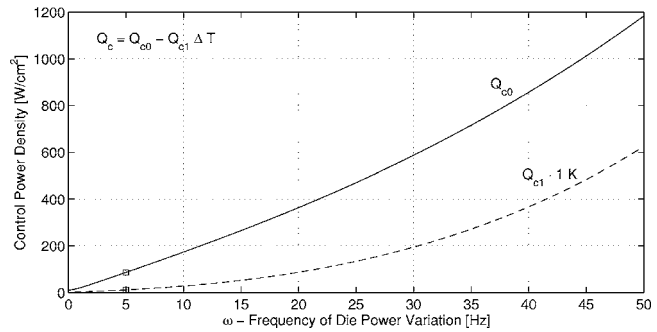


Fig. 4 Control power density for optimal control of a single frequency die power profile with $Q_d=10$ W/cm² and frequencies from zero to 50 Hz

will be limited to optical powers of a few hundred watts or so, facilitating heat fluxes in the range of several hundred watts per square centimeter at most [2,3].

The lower line in Fig. 4 shows the control power that can be saved by allowing the die temperature to fluctuate with a representative peak-to-peak amplitude of $\Delta T=1$ K. This lower line will be the same for all die power densities Q_d since $Q_{c1} \neq f(Q_d)$. The net control power with a fluctuation Q_c in Eq. (26) can be seen to decrease as the allowed tolerance ΔT is increased, a fact that will be important for control of a nonsinusoidal die power profile.

3 Nonsinusoidal Die Power Profiles

The computation of control power profiles for the more realistic case of nonsinusoidal die power is based on the equations derived in the previous section. Instead of using the die power profile defined in Eq. (4), this profile now becomes a series. In general, this may be an infinite series, but significant power will be associated with only the first N terms, where N must be determined on a case by case basis. The die power profile may thus be written as a truncated series

$$q_d(t) = \sum_{n=1}^N (Q_d)_n \cos(\omega_n t + \varphi_n) \quad (30)$$

where n denotes the n th frequency and φ_n its phase shift. The control power profile for this more realistic die power profile is

$$q_c(t) = \sum_{n=1}^N (Q_c)_n \cos(\omega_n t + \varphi_n + \alpha_n) \quad (31)$$

In order to control the die temperature to a prescribed total temperature tolerance, a die temperature profile of the following form is assumed:

$$T_{DIE}(t) = \sum_{n=1}^N \frac{\Delta T_n}{2} \cos(\omega_n t + \varphi_n + \beta_n) \quad (32)$$

The difficulty in controlling a nonsinusoidal die power profile arises from this equation. The prescribed temperature tolerance ΔT is the peak-to-peak amplitude of Eq. (32). There is no a priori basis for dividing this total tolerance among the amplitudes and phase shifts of the individual frequencies ΔT_n . If the individual tolerances ΔT_n are specified, then the corresponding control power for frequency ω_n may be calculated by using the same method as for a single frequency to find $(Q_c)_n$ and α_n . An optimal division of the total tolerance among the component frequencies may be calculated analytically only for certain simple cases, and in general it must be found by numerical iteration.

An upper bound on the amplitude of Eq. (32) is given by

Table 3 Results for square wave die power profile with a prescribed temperature tolerance $\Delta T=2$ K

Frequency	n	1	2	3	4	peak-to-peak amplitude
Control power phase shift	ω_n	5 Hz	15 Hz	25 Hz	35 Hz	
Control power phase shift	α_n	271.45°	292.90°	309.72°	324.84°	
Die temperature phase shift	β_n	330.21°	305.86°	293.91°	287.72°	
Maximal temperature fluctuation	$(\Delta T_{max})_n$	9.77 K	2.17 K	0.90 K	0.48 K	9.62 K
Prescribed temperature tolerance	ΔT_n					
<i>before optimization</i>		0 K	0.62 K	0.90 K	0.48 K	1.94 K
<i>after optimization</i>		0 K	0.69 K	0.90 K	0.48 K	2.00 K
Control power density	$(Q_c)_n$	109.59 W/cm ²	76.76 W/cm ²	0 W/cm ²	0 W/cm ²	371.60 W/cm ²
<i>for control to $\Delta T = 0$ K</i>	$(Q_{c0})_n$	109.59 W/cm ²	112.60 W/cm ²	119.79 W/cm ²	130.14 W/cm ²	

$$\Delta T = \sum_n \Delta T_n \quad (33)$$

which can be used for an initial guess of the temperature tolerances, ΔT_n . Some iteration will usually be necessary to get from this initial guess to the optimal solution. The proposed process of splitting the total temperature tolerance follows from one main conclusion from the previous section: The possible gain in control power for a specific temperature tolerance is larger the higher the frequency. In other words, applying a temperature tolerance to a higher frequency will lead to a larger reduction of the required control power than applying the same temperature tolerance to a lower frequency. Therefore, the following steps will yield an optimized control power profile:

- Sort the frequency data according to their frequencies, ω_n (where $n=1, \dots, N$), starting with the lowest frequency that gets the index $n=1$. Compute the maximal temperature fluctuation for the uncontrolled case $(\Delta T_{max})_n$ for each frequency using Eq. (25).
- The total prescribed temperature tolerance ΔT can now be split into temperature tolerances for each frequency ΔT_n . This can be done using Eq. (33) as follows. The splitting process starts with the highest frequency ($n=N$). If the total prescribed temperature tolerance is larger than the maximal temperature fluctuation for this frequency n , its prescribed temperature tolerance is simply

$$\Delta T_n = (\Delta T_{max})_n \quad (34)$$

and this temperature tolerance is subtracted from the total prescribed temperature tolerance. This step is repeated for the next lower frequency until the remaining total prescribed temperature tolerance is smaller than the maximal temperature fluctuation $(\Delta T_{max})_n$. If that is the case, the temperature tolerance ΔT_n becomes

$$\Delta T_n = \Delta T - \sum_{n+1}^N (\Delta T_{max})_n \quad (35)$$

All remaining lower frequencies have to be controlled to $\Delta T_n=0$ K.

- The control power computed in steps 1 and 2 is too large, because it is based on the upper bound Eq. (32). The actual amplitude of the die temperature can now be computed by evaluating Eq. (32). The difference between the actual amplitude and the prescribed temperature tolerance is then added to the lowest frequency for which $\Delta T_n \neq 0$. This step has to be repeated until the difference is smaller than a desired accuracy ε .

Knowing the temperature tolerances for each frequency n , the required phase shifts α_n and β_n as well as the control power den-

sities, $(Q_c)_n$, can be computed from Eqs. (22)–(24), respectively. The control power profile can be evaluated from Eq. (31).

Comparison of the uncontrolled $(\Delta T)_{max}$ for the highest frequency N in the truncated series to the overall tolerance gives an indication of whether the series has been truncated at too low a value of N . The sensitivity of the result to the chosen N may be checked by changing the value of N .

Example. A square wave die power profile and a triangular wave die power profile are used as dimensional examples for the control of a nonsinusoidal die power profile. The square wave profile can be written as

$$q_d(t) = \frac{4Q}{\pi} \sum_{n=1}^4 \frac{1}{2n-1} \cos\left((2n-1)\omega \cdot 2\pi \cdot t - \frac{\pi}{2}\right) \quad (36)$$

where Q is the amplitude of the square wave¹ and ω its frequency in hertz. The die power profile is assumed to have an amplitude $Q=10$ W/cm² with a frequency of $\omega=5$ Hz. Further properties are given in Tables 1 and 2. Table 3 provides an overview of the results. The first two lines give the phase shifts α_n and β_n and the third line the maximal temperature fluctuations for the uncontrolled case $(\Delta T_{max})_n$. The next two lines are the temperature tolerances ΔT_n before and after the optimization described previously. Note that the prescribed temperature tolerances for the first two frequencies equal the maximal temperature fluctuations for these frequencies. The temperature tolerance for the third frequency is changed during the optimization process to match the actual die temperature magnitude and the prescribed total temperature tolerance with an accuracy $\varepsilon=10^{-4}$ K. The temperature tolerances ΔT_n before the optimization sum up to the prescribed total temperature tolerance ΔT according to Eq. (33) whereas the sum of the temperature tolerances ΔT_n after the optimization is larger than ΔT . The next line gives the control power densities $(Q_c)_n$ after the optimization process. The control power densities for the first two frequencies are zero since these two frequencies are allowed to fluctuate uncontrolled ($\Delta T_n=(\Delta T_{max})_n$). The last line shows the control power densities $(Q_{c0})_n$ that are required to control the die temperature to be constant ($T_{DIE}=0$).

Figure 5 shows the temperature and power profiles for this example. The upper figure shows the convection-side and the back-face temperature profile of the IHS along with the die temperature profile. The lower figure shows the die power and the control power profile. The die power profile has the form of a square wave whereas the control power profile only consists of two frequencies as given in Table 3. The control power necessary to control a single frequency die power profile with the same power density and frequency is, according to Fig. 3, $Q_c=63.64$ W/cm². This control power is about a third of the power required to con-

¹Half the peak-to-peak amplitude.

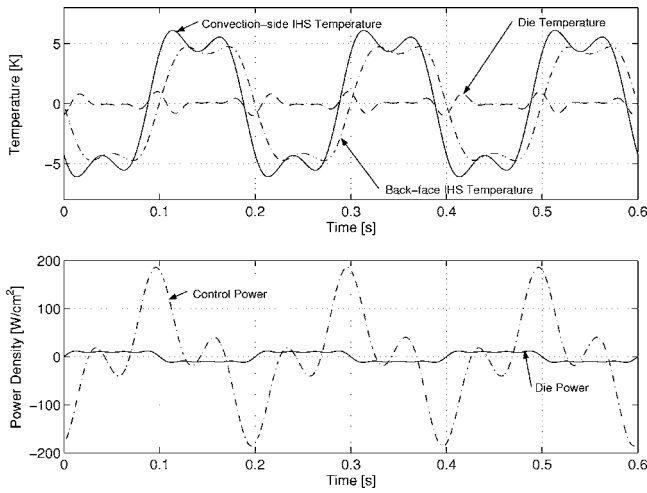


Fig. 5 Temperature and power profiles for square wave die power profile and a prescribed temperature tolerance of $\Delta T = 2$ K. Properties are given in Tables 1 and 2.

control a square wave die power profile. The reason for this large difference can be found in the relatively sharp edges in the square wave die power profile which drive the temperature faster than a sine wave does.

The second example is for a triangular wave die power profile of the form

$$q_d(t) = \frac{8Q}{\pi^2} \sum_{n=1}^4 \frac{1}{(2n-1)^2} \cos\left((2n-1)\omega \cdot 2\pi \cdot t + (-1)^n \frac{\pi}{2}\right) \quad (37)$$

The die power density is again set to $Q_d = 10$ W/cm² and the frequency to $\omega = 5$ Hz. The results for this example are summarized in Table 4. Only the temperature tolerance for lowest frequency ΔT_4 is not equal to its maximal (uncontrolled) temperature fluctuation, $(\Delta T_{\max})_1$, and is changed during the optimization process. The phase shifts α_n and β_n are the same as for the square wave die power profile since they are only dependent on the frequencies ω_n . Figure 6 shows the temperature and power profiles for this example. The required control power of $Q_c = 53.63$ W/cm² is even smaller than for a single frequency die power profile.

4 Summary

The temperature control in a distributed-parameter thermal system presented in [4] has been extended to nonsinusoidal input power profiles. A method for determining the optimal control

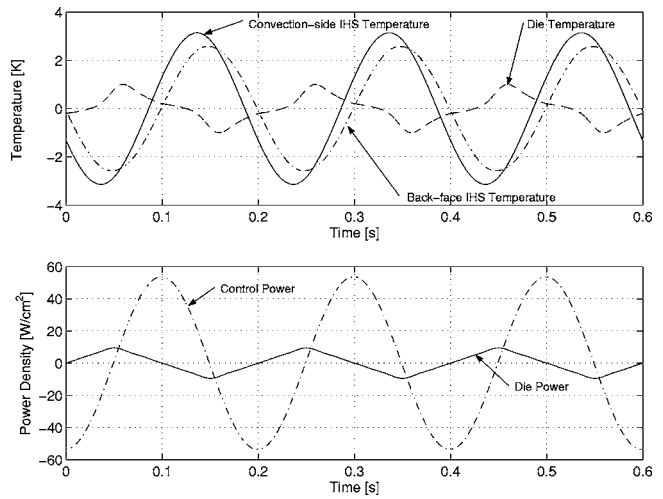


Fig. 6 Temperature and power profiles for triangular wave die power profile and a prescribed temperature tolerance of $\Delta T = 2$ K. Properties are given in Tables 1 and 2.

power has been developed for a single frequency power input and was extended to find the optimal control power profile for nonsinusoidal input power profiles. It is shown that control tolerances should be assigned to the highest frequencies first, so as to limit the total power required. The control power scheme developed in this paper could help to reduce optical laser power and therefore costs for the proposed control method.

Acknowledgment

C.C.R. would like to thank the German Academic Exchange Service and the German National Academic Foundation for financial support of this work. J.H.L. gratefully acknowledges partial support from Teradyne, Inc.

Nomenclature

- A, B, P, R, U, V = Mathematical constants, see the Appendix
- a_t = Thermal diffusivity, m²/s
- Bi_{IHS} = Biot number for top side of IHS $h_c b/k$
- b = IHS thickness, m
- C_1, C_2 = Mathematical constants, Eqs. (10) and (11)
- C_1^*, C_2^* = Mathematical constants, Eq. (21)
- c_1, c_2 = Mathematical constants, Eq. (3)
- c_p = Specific heat capacity at constant pressure, J/kg K
- h_c = Average convective transfer coefficient W/m² K

Table 4 Results for triangular wave die power profile with a prescribed temperature tolerance $\Delta T = 2$ K

	n	1	2	3	4	peak-to-peak amplitude
Frequency	ω_n	5 Hz	15 Hz	25 Hz	35 Hz	
Control power phase shift	α_n	271.45°	292.90°	309.72°	324.84°	
Die temperature phase shift	β_n	330.21°	305.86°	293.91°	287.72°	
Maximal temperature fluctuation	$(\Delta T_{\max})_n$	6.22 K	0.46 K	0.11 K	0.04 K	6.70 K
Prescribed temperature tolerance	ΔT_n					
<i>before optimization</i>		1.38 K	0.46 K	0.11 K	0.04 K	1.95 K
<i>after optimization</i>		1.44 K	0.46 K	0.11 K	0.04 K	2.00 K
Control power density	$(Q_c)_n$	53.63 W/cm ²	0 W/cm ²	0 W/cm ²	0 W/cm ²	107.26 W/cm ²
<i>for control to $\Delta T = 0$ K</i>	$(Q_{c0})_n$	69.77 W/cm ²	23.89 W/cm ²	15.25 W/cm ²	11.84 W/cm ²	

i = The imaginary number $\sqrt{-1}$
 k = Thermal conductivity, W/m K
 L = Unsteady diffusion scale in IHS $\sqrt{\omega/2a_t}$, 1/m
 m = Die mass per unit area, kg/m²
 n = Index for nonsinusoidal die power profiles
 Q_{BF} = Power density of heat flux from die into IHS, Eq. (17), W/m²
 Q_c = Control power density, W/m²
 Q_{c0} = Constant part of control power for optimal control case, Eq. (27), W/m²
 Q_{c1} = Linear coefficient of control power for optimal control case, Eq. (28), W/m² K
 Q_d = Die power density, W/m²
 $q_{BF}(t)$ = Heat flux from die into IHS, Eq. (16), W/m²
 $q_c(t)$ = Control power flux, Eqs. (5) and (31), W/m²
 $q_d(t)$ = Die power flux, Eqs. (4) and (30), W/m²
 R_t = Thermal contact resistance, K m²/W
 $T_{BF}(t)$ = Back-face IHS temperature, Eq. (6), K
 $T_{DIE}(t)$ = Die temperature, K
 ΔT = Prescribed temperature tolerance, K
 ΔT_{max} = Maximal temperature fluctuation for uncontrolled case, Eq. (25), K
 t = Time, s
 $W(x, t)$ = Complex temperature solution, Eq. (1)
 $X(x)$ = Real part of complex temperature solution, K
 x = Distance from convection-side of IHS, m

Greek Symbols

$\alpha, \beta, \gamma, \varphi$ = Phase shifts, rad
 λ = Lumped frequency response of die $1/mc_p R_t$, 1/s
 ω = Frequency of die power variation, rad/s

Appendix: Mathematical Constants

The following mathematical constants are taken from [4]:

$$\begin{aligned}
 A &= \frac{Bi_{IHS}}{bL} \cos(bL)(e^{2bL} + 1) - [\cos(bL) + \sin(bL)] \\
 &\quad + e^{2bL}[\cos(bL) - \sin(bL)] \\
 B &= \frac{Bi_{IHS}}{bL} \sin(bL)(e^{2bL} - 1) - [\cos(bL) - \sin(bL)] \\
 &\quad + e^{2bL}[\cos(bL) + \sin(bL)] \\
 P &= e^{bL}[\cos(bL) - \sin(bL)] - \frac{e^{-bL}}{D}[G \cos(bL) + N \sin(bL)] \\
 R &= e^{bL}[\sin(bL) + \cos(bL)] + \frac{e^{-bL}}{D}[G \sin(bL) - N \cos(bL)] \\
 U &= \frac{P \cdot E + R \cdot F}{D} \\
 V &= \frac{P \cdot F - E \cdot R}{D}
 \end{aligned}$$

where

$$\begin{aligned}
 D &= h_c^2 + 2h_c kL + 2(kL)^2 \\
 E &= 2(kL)^2 - h_c^2 \\
 \text{and } F &= 2h_c kL
 \end{aligned}$$

References

- [1] Pfahnl, A. C., Lienhard, V. J. H., and Slocum, A. H., 1999, "Thermal Management and Control in Testing Packaged Integrated Circuit (IC) Devices," *Proc. 34th Intersociety Energy Conversion Conf.*, paper no. 1999-01-2723.
- [2] Sweetland, M., Lienhard, V. J., and Slocum, A. H., 2005, "A Convection/Radiation Temperature Control System for High Power Density Electronic Device Testing" (unpublished).
- [3] Sweetland, M., 2001, *Design of Thermal Control Systems for Testing of Electronics*, PhD thesis, Massachusetts Institute of Technology, Cambridge, MA.
- [4] Sweetland, M., and Lienhard, V. J. H., 2003, "Active Thermal Control of Distributed Parameter Systems With Application to Testing of Packaged (IC) Devices," *ASME J. Heat Transfer*, **125**, pp. 165–174.
- [5] Richter, C. C., 2004, "Active Thermal Control of Distributed Parameter Systems Excited at Multiple Frequencies," Diplomarbeit, Massachusetts Institute of Technology, Cambridge, MA.
- [6] Baehr, H. D., and Stephan, K., 2004, *Wärme und Stoffübertragung*, Springer, Berlin.